Int. J. Solids Structures Vol. 25, No. 2, pp. 201-211, 1989
Printed in Great Britain.

0020-7683/89 $3.00 + .00

A DIRECT VECTOR SIMULATION FOR THE ANALYSES OF NODAL AND UNDULATING ELASTICA

SUNIL SAIGAL† and W. A. KISTLER
Mechanical Engineering Department, Worcester Polytechnic Institute, Worcester, MA 01609, U.S.A.

(*Received* 16 *December* 1987; *in revised form* 30 *September* 1988)

Abstract—A non-linear vector equilibrium/constitutive differential equation governing an elastica is directly simulated without decomposition. The solution is obtained using repeated applications of a truncated Taylor's expansion to advance along the elastica. Lacking a vector data type in Fortran 77, the complex data type is used for direct two-dimensional simulations. Rapid convergence and good accuracy are observed for sufficiently small increments using single precision. Numerical results for both nodal and undulating elastica are presented. Good agreement is shown with existing alternative solutions.

INTRODUCTION

The finite deflection of uniform beams may be obtained using the Euler–Bernoulli law of bending. The approximate solutions, in series form, of a uniform, initially straight cantilever, loaded with a single vertical force at the free end, have been given by Boyd (1924) and by Gross and Lehr (1938). The exact, closed-form solutions were given by Barten (1944) and in the elliptic function form by Bisshopp and Drucker (1945). The solution of elastica using the principle of elastic similarity was developed by Frisch-Fay (1961a, b, 1962a) who applied it to some cantilever cases. By integrating the Bernoulli–Euler equation, Frisch-Fay (1962b) also gave another closed-form solution of a cantilever with two vertical forces. The exact solution for a straight bar on unyielding knife-edged supports, without and including friction was given by Frisch-Fay (1962b). The same problem, without friction, was solved by Freeman (1946), Wijngaarden (1946), Conway (1947), and Gospodnetic (1959). The finite deflection of a centrally loaded bar supported by two pivoted end links were obtained by Gorski (1974). Numerical analysis for such problems has been performed by Seames and Conway (1957), Wang *et al.* (1961), Wang (1969), and Yang (1973). Numerous finite element solutions for such problems are available and a brief account was given by Yang and Saigal (1984). Saje and Srpcic (1985) recently presented a large deformation beam theory based on the uniaxiality of the strain tensor.

The solutions presented in the literature mentioned above are complicated by several substitutions and transformations required which tend to obscure the physical nature of the problem. The formulations for these solutions are based on equations of equilibrium written in terms of the individual displacement components. In this paper a straightforward procedure, for which the equations of equilibrium are both expressed and solved directly in their vector form, is presented. The position vector for a point on the elastica is expressed in terms of a Taylor's series expansion about a neighboring point on the elastica. An incremental marching procedure is then used to advance along the entire length of the elastica. The complex data type capabilities are used in programming on the computer for the solution of two-dimensional equilibrium equations directly in their vector form. The present method is applicable to both nodal and undulating elastica. Numerical examples are presented and compared with existing alternative results to demonstrate the effectiveness of the present method. A good convergence of the series for solving large displacement problems is seen.

† Author to whom all correspondence should be addressed.

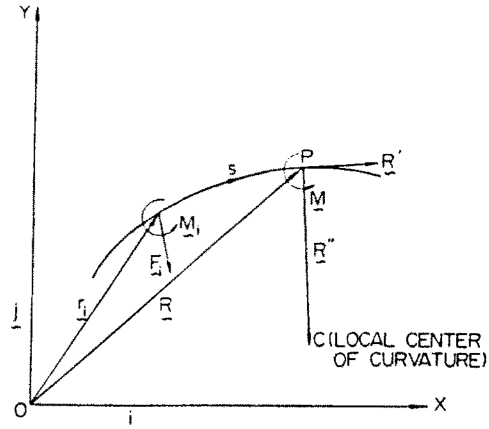

Fig. 1. The elastic curve.

THE GOVERNING VECTOR EQUATIONS

For the elastic curve shown in Fig. 1, let the distance along the curve s be the independent variable and the position vector **R** to point P be the dependent variable. The derivative

$$\mathbf{R}' = \frac{d\mathbf{R}}{ds} \tag{1}$$

is the local unit tangent directed in the positive s-direction. The second derivative $\mathbf{R}''$ has the local curvature $(1/\rho)$ as its magnitude and is directed towards the local center of curvature C. The governing equation for the elastica then becomes

$$\mathbf{R}'' = \mathbf{R}' \times \frac{\mathbf{M}}{EI} \tag{2}$$

where **M** is the local bending moment at point P, EI the bending rigidity, and the cross (×) denotes the vector cross product. It is noted that eqn (2) is independent of the vector coordinate system. A linearly elastic material is assumed which, if anisotropic, has a principal axis coincident with the axis of the elastica. It is also assumed that neither is the neutral surface appreciably warped due to the effects of Poisson's ratio nor is any cross-sectional surface appreciably warped due to the effects of local transverse shear.

The local bending moment can be expressed as a summation of cross products

$$\mathbf{M} = \sum_i [(\mathbf{r}_i - \mathbf{R}) \times \mathbf{F}_i - \mathbf{M}_i] \tag{3}$$

where $\mathbf{F}_i$ and $\mathbf{M}_i$ are the force and bending moment, respectively, in any direction acting on a point on the elastica corresponding to the position vector $\mathbf{r}_i$.

SERIES SOLUTION

The solution for the position vector $\mathbf{R}(s+\Delta s)$ can be expressed by using Taylor's series expansion as

$$\mathbf{R}(s+\Delta s) = \sum_{n=0}^{\infty} \mathbf{R}^n(s)\frac{(\Delta s)^n}{n!} \tag{4}$$

$$\mathbf{R}'(s+\Delta s) = \sum_{n=1}^{\infty} \mathbf{R}^n(s)\frac{(\Delta s)^{(n-1)}}{(n-1)!} \tag{5}$$

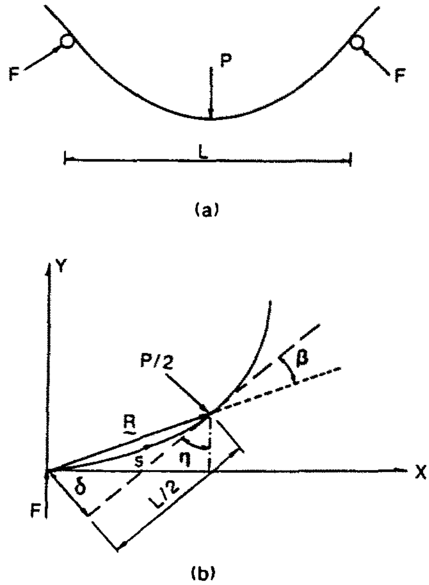

Fig. 2. An initially straight beam on frictionless knife-edged supports under a central load P.

where Δs is the incremental distance along the elastic curve, and $\mathbf{R}^n(s)$ denotes the nth derivative of $\mathbf{R}(s)$ with respect to s and can be obtained by successive differentiation of eqn (2). The truncation point of eqns (4) and (5) depends on the behavior of the higher order derivatives. If the expansion are truncated with an inadequate number of terms, the requisite mesh size for a desired accuracy becomes so small that it is never accomplished in single precision due to roundoff errors. Also, execution time becomes excessive. For all of the examples presented in this study, truncation of eqns (4) and (5) at $n = 6$ was found to yield adequate accuracy with reasonably short execution times.

SOLUTION PROCEDURE

For all the simulations which can be cast as initial value problems, and all of the examples which follow can be so treated, the solution procedure begins at $s = 0$ where the boundary conditions are known. The method then proceeds in increments Δs of the independent variable s along the elastic curve until the entire curve is spanned. Successively smaller values of Δs are chosen until the simulation results become insensitive to further reductions in Δs. The end of a curve is identified by the boundary condition at that point. Shooting methods, which are iterative in nature, are employed to determine the point satisfying this boundary condition. This procedure is demonstrated in the following sections for large displacements of elastic beams under various loading and boundary conditions.

A. *Straight beam on frictionless unyielding knife-edged supports*

Consider a straight beam supported on frictionless knife-edged supports under a central load as shown in Fig. 2(a). Although the actual length of the beam lying between fixed supports varies with the deflection curve, the length L is defined as the distance between the supports. Thus, the length and center deflection, as defined, do not vary simultaneously.

Substituting eqn (3), for a single force and for $\mathbf{r}_i = 0$, into eqn (2), we have

$$EI\mathbf{R}'' = (\mathbf{R} \times \mathbf{F}) \times \mathbf{R}'. \tag{6}$$

The dimensionless parameter is defined as

$$\boldsymbol{\theta} = \left(\frac{F}{EI}\right)^{1/2} \mathbf{R} \tag{7}$$

and the dimensionless independent variable as

$$\alpha = \left(\frac{F}{EI}\right)^{1/2} s. \tag{8}$$

Using these definitions we obtain

$$\frac{d\mathbf{R}}{ds} = \frac{d\boldsymbol{\theta}}{d\alpha} = \boldsymbol{\theta}' \tag{9}$$

$$\frac{d^2\mathbf{R}}{ds^2} = \left(\frac{F}{EI}\right)^{1/2} \frac{d^2\boldsymbol{\theta}}{d\alpha^2} = \left(\frac{F}{EI}\right)^{1/2} \boldsymbol{\theta}''. \tag{10}$$

Governing eqn (6), using eqns (9) and (10) can be written in dimensionless form as

$$\boldsymbol{\theta}'' = (\boldsymbol{\theta} \times \mathbf{j}) \times \boldsymbol{\theta}' \tag{11}$$

with the boundary conditions

$$\boldsymbol{\theta}(0) = 0 \quad \text{and} \quad \boldsymbol{\theta}'(0) = \mathbf{i} \tag{12}$$

where $\mathbf{i}, \mathbf{j}, \mathbf{k}$ are the unit vectors in the coordinate directions x, y, and z, respectively.

Also, from Fig. 2(b), we have

$$P = 2F \sin \eta = 2F\mathbf{R}' \cdot \mathbf{i} \tag{13}$$

$$\delta = R \sin \beta = \frac{\mathbf{R} \times \mathbf{R}'}{R} \tag{14}$$

since the curve is two-dimensional, and

$$L = 2R \cos \beta = 2\mathbf{R} \cdot \mathbf{R}'. \tag{15}$$

Using eqns (7)–(15), we obtain

$$\frac{PL^2}{EI} = 8(\boldsymbol{\theta}' \cdot \mathbf{i})(\boldsymbol{\theta} \cdot \boldsymbol{\theta}')^2 \tag{16}$$

and

$$\frac{\delta}{L} = \frac{1}{2R} \frac{\boldsymbol{\theta} \times \boldsymbol{\theta}'}{\boldsymbol{\theta} \cdot \boldsymbol{\theta}'}. \tag{17}$$

The solution procedure starts at $\alpha = 0$ (corresponding to the origin of Fig. 2(b) which is at a beam support) with the boundary conditions given by eqn (12). The iterative solution proceeds in increments of $\Delta\alpha$ using eqn (11) and its derivatives substituted into the dimensionless forms of eqns (4) and (5). At the end of each iteration, the dimensionless position vector $\boldsymbol{\theta}$ can be interpreted as representing the midpoint location of a new beam for which the dimensionless load and deflection are $p = PL^2/EI$ and δ/L, respectively, as

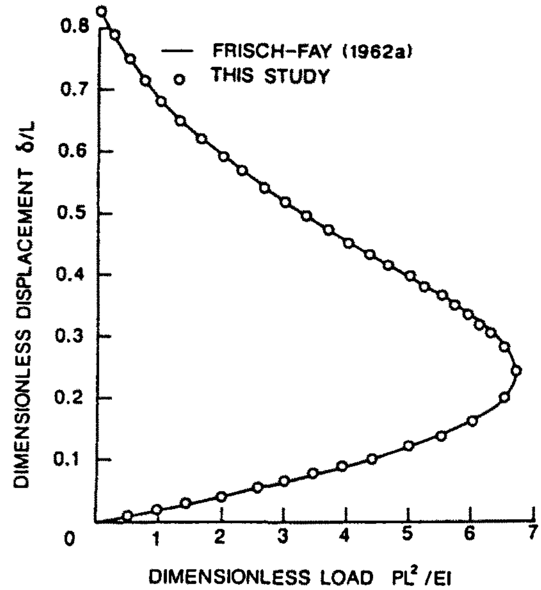

Fig. 3. Load-deflection curve for centrally loaded beam on frictionless knife-edged supports.

defined in eqns (16) and (17). Thus, each iteration produces a new plotted point for Fig. 3. This problem was earlier studied by Frisch-Fay (1962a) for nodal elastica and his results are plotted in Fig. 3 for comparison. A good agreement of results is seen. For the present study, the solution was further extended. Multiple segments of the load-deflection curve were obtained for each quadrant and some initial segments are shown in Fig. 4.

Several deflection profiles corresponding to the curve in Fig. 4 are shown in Figs 5–8. The elastic beam sags under the load acting downward until a self-supporting deflection profile is obtained corresponding to $p = 0$. The load is then applied in the reverse (upward) direction to maintain the beam in equilibrium. As the solution marches further, interfering deflection profiles are obtained as shown in Fig. 6. These deflection profiles corespond to the load-deflection segment in the third quadrant. On further increasing α, undulating curves involving inflection points are obtained as shown in Fig. 7. The points corresponding

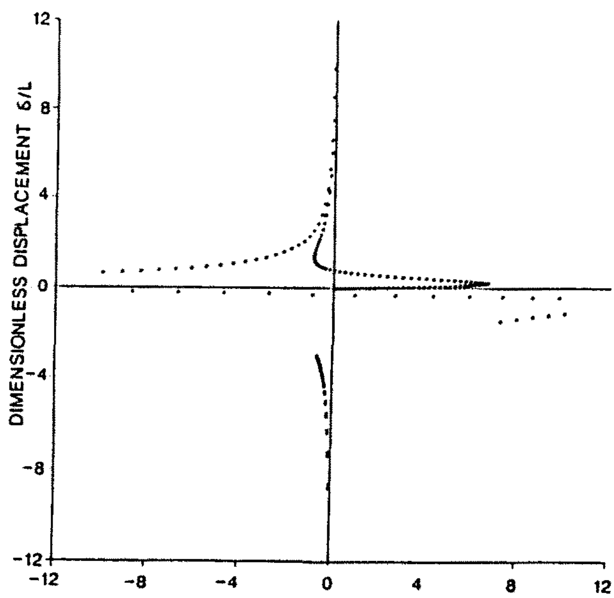

Fig. 4. Multiple segments of the load-deflection curve for centrally loaded beam on frictionless knife-edged supports.

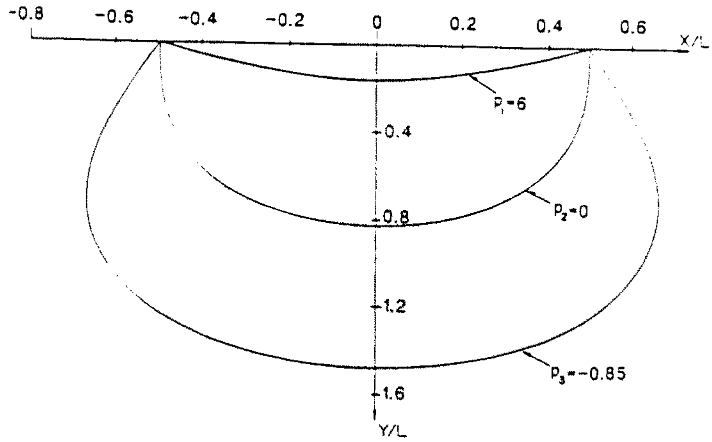

Fig. 5. Deflection profiles for $p = 6, 0$, and -0.85, respectively.

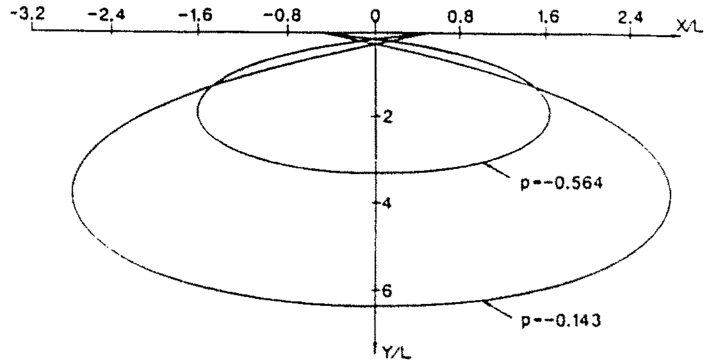

Fig. 6. Deflection profiles for $p = -0.564$ and -0.143, respectively.

to $p = 6.69$ and 29.05 lie in the second quadrant while the point for $p = 4.34$ lies on the next segment in the third quadrant. These load values signify the load that must be applied to maintain the beam in equilibrium if the beam is deflected in the shape of the deflection profiles shown in Fig. 7. Finally deflection profiles corresponding to a segment in the fourth quadrant of Fig. 4 are shown in Fig. 8. The elastic curves obtained are interfering undulating elastica.

B. *Cantilever beam with normal force at free end*

This situation is identical to Case A above with the addition of a coordinate transformation and a redefinition of some of the parameters (see inset on Fig. 9). The midbeam point and the local normal for Case A become the "wall" for this case, the old load F

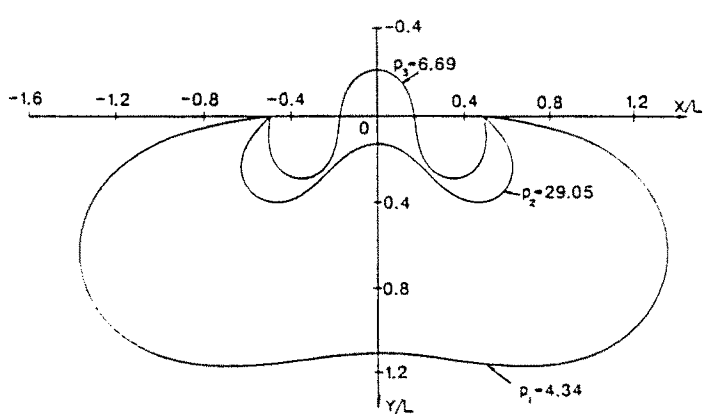

Fig. 7. Deflection profiles in the third quadrant for $p = 6.69$, 29.05, and 4.34, respectively.

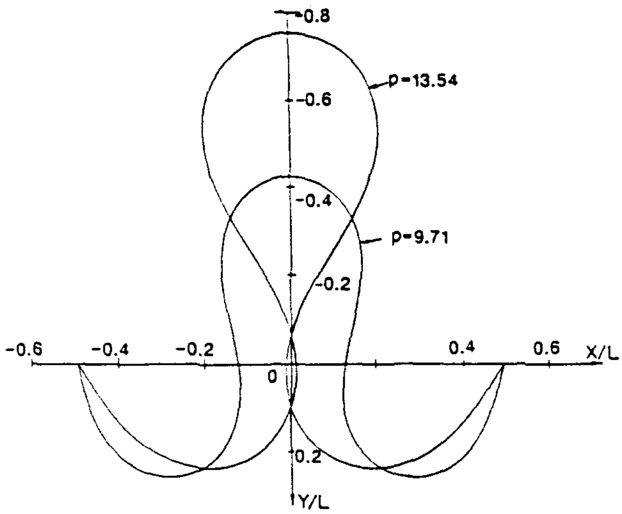

Fig. 8. Deflection profiles in the fourth quadrant for $p = 9.71$ and 13.54, respectively.

becomes the new load P and the new L is the actual beam length obtained by integrating along the beam during the iteration process. The initial conditions are the same, and, as before, each iteration yields dimensionless data which can be interpreted as decribing the behavior of either a new beam or the same beam under different loading conditions.

Note the following equivalences: either of the curves in Fig. 6 is approximately equivalent to the curve for load p_1 in Fig. 10; the curves for loads p_2 and p_3 in Fig. 7 are approximately equivalent to the curves for loads p_2 and p_3, respectively, in Fig. 10. This problem has been studied earlier by Saje and Srpcic (1985) and their solutions are also plotted in Figs 9 and 10 for comparison. A good agreement in results is seen.

C. *Cantilever beam with moment at free end*

This case is included to provide a simple test of the iteration error which necessarily accumulates during the simulation process. Governing eqn (2) is simplified by the condition that the bending moment is constant.

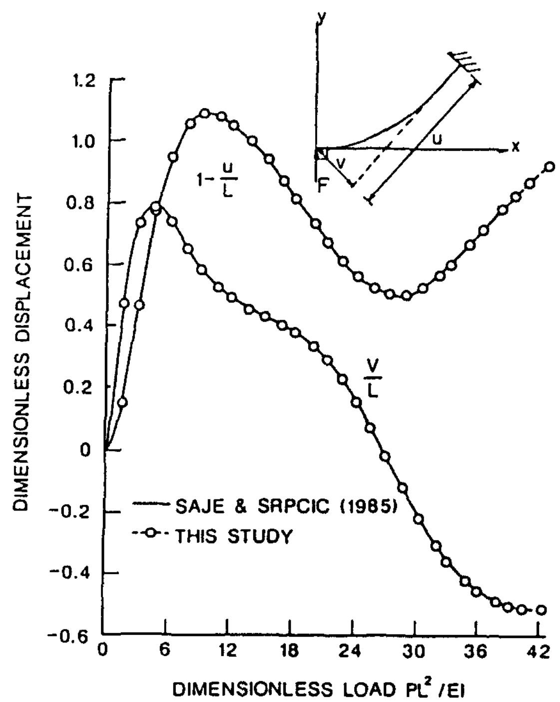

Fig. 9. Load–deflection curve for cantilever beam with normal force at free end.

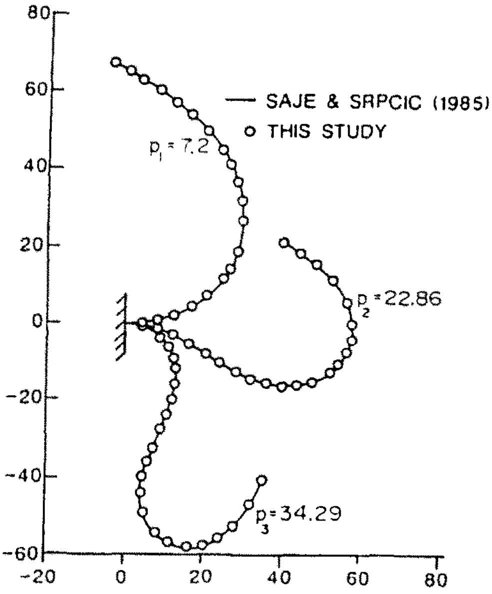

Fig. 10. Deflection profiles for cantilever beam with normal force at free end.

The following transformations are introduced:

$$\boldsymbol{\theta} = \frac{M}{EI}\mathbf{R} \tag{18}$$

$$\alpha = \frac{M}{EI}s \tag{19}$$

where α is the dimensionless independent variable that is incremented in steps to obtain the solution. The governing equation is then written in dimensionless form as

$$\boldsymbol{\theta}'' = \mathbf{k}\times\boldsymbol{\theta}' \tag{20}$$

where **k**, as before, is the unit vector in the z-direction.

As a test the simulation was iterated for an entire circle and the discrepancy between the initial point and the final point was investigated. The resulting relative error was defined as the absolute discrepancy divided by the integrated circumference along the circle which, itself, was checked against the theoretical circle diameter.

The most convenient boundary conditions are those for Cases A and B

$$\boldsymbol{\theta}(0) = 0 \quad \text{and} \quad \boldsymbol{\theta}'(0) = \mathbf{i}.$$

The results are shown in Table 1. Note that carrying three derivative orders in the simulation yields a relative accuracy of approximately four significant figures, whereas, when five derivative orders are carried, the machine error in single precision completely masks the simulation error.

D. *Cantilever beam with vertical force at free end*

A cantilever beam with a concentrated vertical force at its free end is considered next. From Fig. 11

$$\mathbf{M} = -\mathbf{M}_0 - \mathbf{R}\times\mathbf{F}_0 \tag{21}$$

and the elastic beam equation can be written as

Table 1. Cantilever with moment at free end

x (deg)	Simulated θ_x	Simulated θ_y	Exact θ_x	Exact θ_y	δ Simulation error
		Case I: $N = 60$, $M = 3$, $L = 3$			
0.00000	0.00000	0.00000	0.00000	0.00000	0.00000
18.000	0.30901	0.48958E−01	0.30902	0.48943E−01	0.15029E−04
36.000	0.58777	0.19101	0.58779	0.19098	0.30046E−04
54.000	0.80898	0.41224	0.80902	0.41221	0.45094E−04
72.000	0.95100	0.69101	0.95106	0.69098	0.60164E−04
90.000	0.99993	1.0000	1.0000	1.0000	0.75179E−04
108.00	0.95097	1.3090	0.95106	1.3090	0.90215E−04
126.00	0.80893	1.5877	0.80902	1.5878	0.10527E−03
144.00	0.58771	1.8089	0.58779	1.8090	0.12033E−03
162.00	0.30896	1.9509	0.30902	1.9511	0.13541E−03
180.00	−0.22626E−04	1.9999	−0.32584E−06	2.0000	0.15047E−03
198.00	−0.30898	1.9509	−0.30902	1.9511	0.16550E−03
216.00	−0.58769	1.8089	−0.58779	1.8090	0.18058E−03
234.00	−0.80887	1.5877	−0.80902	1.5878	0.19550E−03
252.00	−0.95086	1.3089	−0.95106	1.3090	0.21044E−03
270.00	−0.99978	0.99998	−1.0000	1.0000	0.22544E−03
288.00	−0.95082	0.69104	−0.95106	0.69098	0.24045E−03
306.00	−0.80880	0.41235	−0.80902	0.41221	0.25547E−03
324.00	−0.58761	0.19119	−0.58778	0.19098	0.27043E−03
342.00	−0.30891	0.49207E−01	−0.30902	0.48943E−01	0.28541E−03
360.00	0.25168E−04	0.29949E−03	0.16054E−05	0.12886E−11	0.30041E−03
					$\frac{\delta_{max}}{C} = 4.78 \times 10^{-3}$
		Case II: $N = 60$, $M = 3$, $L = 5$			
0.00000	0.00000	0.00000	0.00000	0.00000	0.00000
18.000	0.30902	0.48943E−01	0.30902	0.48943E−01	0.74506E−08
36.000	0.58779	0.19098	0.58779	0.19098	0.00000
54.000	0.80902	0.41221	0.80902	0.41221	0.59605E−07
72.000	0.95106	0.69098	0.95106	0.69098	0.00000
90.000	1.0000	1.0000	1.0000	1.0000	0.11921E−06
108.00	0.95106	1.3090	0.95106	1.3090	0.59605E−07
126.00	0.80902	1.5878	0.80902	1.5878	0.13328E−06
144.00	0.58779	1.8090	0.58779	1.8090	0.59605E−07
162.00	0.30902	1.9511	0.30902	1.9511	0.14901E−06
180.00	−0.82275E−07	2.0000	−0.32584E−06	2.0000	0.24357E−06
198.00	−0.30902	1.9511	−0.30902	1.9511	0.29802E−06
216.00	−0.58779	1.8090	−0.58779	1.8090	0.32098E−06
234.00	−0.80902	1.5878	−0.80902	1.5878	0.50926E−06
252.00	−0.95106	1.3090	−0.95106	1.3090	0.59605E−06
270.00	−1.0000	1.0000	−1.0000	1.0000	0.69765E−06
288.00	−0.95106	0.69098	−0.95106	0.69098	0.84714E−06
306.00	−0.80902	0.41221	−0.80902	0.41221	0.94243E−06
324.00	−0.58779	0.19098	−0.58778	0.19098	0.11309E−05
342.00	−0.30902	0.48943E−01	−0.30902	0.48943E−01	0.13114E−05
360.00	0.16765E−06	−0.40461E−06	0.16054E−05	0.12886E−11	0.14936E−05
					$\frac{\delta_{max}}{C}$ 2.38 × 10^{-7}

N = No. of iterations in full circle.
M = No. of iterations per output.
L = No. of derivative orders taken.

$$EI\mathbf{R}'' = \mathbf{M} \times \mathbf{R}'$$
$$= -\mathbf{R}' \times (\mathbf{M}_0 + \mathbf{R} \times \mathbf{F}_0). \tag{22}$$

The non-dimensional parameters are

$$\alpha = \left(\frac{F_0}{EI}\right)^{1/2} s, \quad \theta = \left(\frac{F_0}{EI}\right)^{1/2} \mathbf{R}$$

and

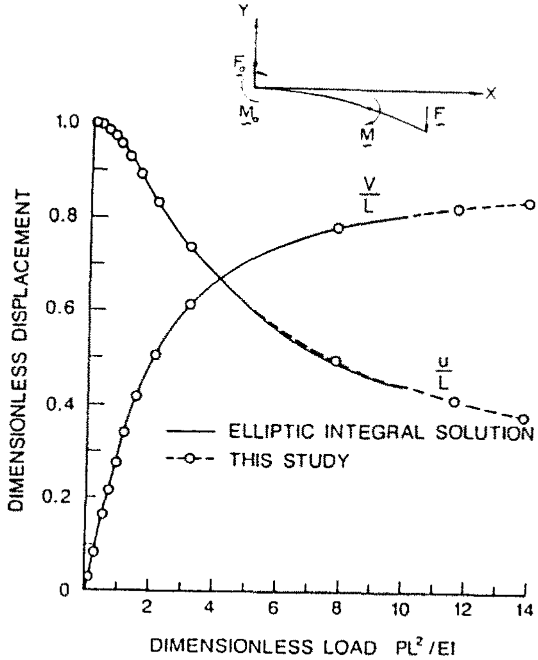

Fig. 11. Load–deflection curve for cantilever beam with vertical force at free end.

$$\beta = \frac{M_0}{(F_0 EI)^{1/2}} \tag{23}$$

where α is the dimensionless independent variable. Equilibrium eqn (22) can then be written as

$$\boldsymbol{\theta}'' = (\beta \mathbf{k} + \boldsymbol{\theta} \times \mathbf{j}) \times \boldsymbol{\theta}'$$

with the boundary conditions

$$\boldsymbol{\theta}(0) = 0 \quad \text{and} \quad \boldsymbol{\theta}'(0) = \mathbf{i}.$$

The non-dimensional deflection and load values are obtained as

$$\frac{\delta_f}{L} = \frac{\boldsymbol{\theta}_f \cdot \mathbf{j}}{\alpha_f}$$

and

$$\frac{FL^2}{EI} = \alpha_f^2$$

where $\boldsymbol{\theta}_f$ and δ_f are the values of $\boldsymbol{\theta}$ and δ at the free end.

For a given value of β and selected values for $\Delta\alpha$ and tolerance ε, the marching procedure starts with the boundary conditions at $\alpha = 0$ until the following condition corresponding to the free end is satisfied:

$$\boldsymbol{\theta}' \times \boldsymbol{\theta}'' = 0. \tag{24}$$

The α value corresponding to this condition was found using an iterative secant search root-finding procedure. In the present two-dimensional analysis, the quantity $(\boldsymbol{\theta}' \times \boldsymbol{\theta}'')$ is a scalar and, thus, the condition given by eqn (24) simplifies the root-finding procedure. The condition, $\theta'' = 0$, is, however, a sufficient criterion. The load–deflection curves for both horizontal and vertical deflections are shown in Fig. 11. The elliptical integral solution due to Bisshopp and Drucker (1945) is also plotted in Fig. 11 for comparison and a good agreement is seen.

CONCLUSIONS

A straightforward numerical procedure for finite deflections of deep elastic beams is presented. The formulation involves writing the equilibrium equations in vector notation. These equations are then solved directly in their vector form without the need to decompose them into their individual component scalar equations. The solution is expressed as a Taylor's series expansion about a known point. The solution procedure is an incremental marching scheme which starts from the known boundary conditions and proceeds along the elastic curve using the series expansion. Numerical results are obtained for an elastic beam on knife-edged fixed supports; and for a cantilever under a normal force, a moment, and a vertical force, respectively, at its free ends. The results obtained are in good agreement with existing alternative solutions which demonstrates the accuracy of the present work. This procedure is especially attractive due to its simplicity. It does not involve numerous substitutions and transformations which have, in earlier solutions, masked the physical nature of the problem. A three-dimensional analysis of elastica should prove to be no more difficult than it is in two dimensions using the current scheme. The coding using Fortran, however, will be more complicated due to the lack of a vector data type.

Acknowledgements—The authors would like to thank Prof. D. N. Zwiep, Head of the Mechanical Engineering Department, Worcester Polytechnic Institute, for his encouragement and support.

REFERENCES

Barten, H. J. (1944). On the deflection of a cantilever beam. *Q. Appl. Math* **2**, 168–171. Correction **3**, 275–276.

Bisshopp, K. E. and Drucker, D. C. (1945). Large deflections of cantilever beams. *Q. Appl. Math.* **3**, 272–275.

Boyd, J. E. (1924). *Strength of Materials*. McGraw-Hill, New York.

Conway, H. D. (1947). The large deflection of simply supported beams. *Phil. Mag.* **38**, 905–911.

Freeman, J. G. (1946). Mathematical theory of deflection of beams. *Phil. Mag.* **37**, 855–862.

Frisch-Fay, R. (1961a). The analysis of a vertical and horizontal cantilever under uniformly distributed load. *J. Franklin Inst.* **271**, 192–199.

Frisch-Fay, R. (1961b). A new approach to the analysis of the deflection of thin cantilevers. *J. Appl. Mech.* **28**, 87–90.

Frisch-Fay, R. (1962a). *Flexible Bars*. Butterworth, London.

Frisch-Fay, R. (1962b). Large deflections of a cantilever under two concentrated loads. *J. Appl. Mech.* **29**, 200–201.

Gorski, W. (1974). Finite elastic deflections of a centrally supported bar supported by two pivoted links. *J. Mech. Engng Sci.* **16**, 317–321.

Gospodnetic, D. (1959). Deflection curve of a simply supported beam. *J. Appl. Mech.* **26**, 675–676.

Gross, S. and Lehr, E. (1938). *Die federn*. V.D.I. Verlag, Berlin.

Saje, M. and Srpcic, S. (1985). Large deformations of in-plane beams. *Int. J. Solids Structures* **21**, 1181–1195.

Seames, A. E. and Conway, H. D. (1957). A numerical procedure for calculating the large deflections of straight and curved beams. *J. Appl. Mech.* **24**, 289–294.

Wang, T. M. (1969). Nonlinear bending of beams with uniformly distributed loads. *Int. J. Non-linear Mech.* **4**, 389–395.

Wang, T. M., Lee, S. L. and Zienkiewicz, O. C. (1961). A numerical analysis of large deflection of beams. *Int. J. Mech. Sci.* **3**, 219–228.

Wijngaarden, A. V. (1946). Large distortions of circular rings and straight rods. *Proc. K. Ned. Adad. Wet., Amsterdam* **49**, 648–664.

Yang, T. Y. (1973). Matrix displacement solution to elastica problems of beams and frames. *Int. J. Solids Structures* **9**, 829–842.

Yang, T. Y. and Saigal, S. (1984). A simple element for static and dynamic response of beams with material and geometric nonlinearities. *Int. J. Numer. Meth. Engng* **20**, 851–867.